Hemi-Labile Ligands in Organolithium Chemistry: Rate Studies of the LDA-Mediated α- and β-Metalations of Epoxides

Antonio Ramírez and David B. Collum*

Contribution from the Department of Chemistry and Chemical Biology, Baker Laboratory, Cornell University, Ithaca, New York 14853-1301

Received June 24, 1999

Abstract: Lithium diisopropylamide (LDA)-mediated α- and β-eliminations of epoxides are described. A comparison between LDA/*n*-BuOMe mixtures and LDA/$MeOCH_2CH_2NMe_2$ (LDA/**3**) mixtures reveals that the LDA dimer solvated by the "hemi-labile" amino ether **3** imparts dramatic rate accelerations, alters relative efficacies of monomer- and dimer-based metalations, and influences the partitioning between α- and β-metalation. The α-elimination of *exo*-norbornene oxide by LDA/*n*-BuOMe and LDA/**3** proceeds exclusively via a dimer-based pathway with a transition structure, $[(R_2NLi)_2(epoxide)(ligand)]^‡$. The β-elimination of tetramethylethylene oxide by LDA/*n*-BuOMe and LDA/**3** proceeds exclusively via a monomer-based pathway with a transition structure, $[(R_2NLi)(epoxide)(ligand)]^‡$. *cis*-Cyclooctene epoxide reacts with LDA/**3** to give two products: (1) a bicyclooctanol derived from an α-metalation and a dimer-based transition structure, $[(R_2NLi)_2(epoxide)(ligand)]^‡$, and (2) 2-cycloocten-1-ol derived from both a monomer-based transition structure, $[(R_2NLi)(epoxide)(ligand)]^‡$, and a dimer-based transition structure, $[(R_2NLi)_2(epoxide)(ligand)]^‡$. Possible geometries of the transition structures are discussed. Hemi-labile ligands that chelate lithium only at the rate-limiting transition structures maximize both the reaction rates and the mechanistic transparency.

Introduction

Difunctional ligands containing both weakly and strongly coordinating appendages, so-called hemi-labile ligands, have received considerable attention in the transition metal literature.[1] Dissociating the weakly ligating group affords coordinatively unsaturated metal centers at a relatively low energetic cost (eq 1).

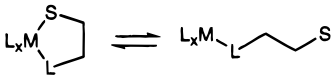

(1)

Although one might question the merits of using chelating ligands in the first place, hemi-labile ligands appear to offer advantages over their monodentate or other bidentate counterparts in some cases.[2]

In contrast, hemi-labile ligands have received no explicit[3] attention in organolithium chemistry. This may be due to the generally limited development of the coordination chemistry of lithium and to the belief that ligand dissociations are not important. However, reactions in which the rate-limiting transition structures are more highly solvated than the reactants offer ideal opportunities to exploit hemi-labile ligands. This is easily envisioned by simply reversing the logic: a difunctional ligand that forms a weakly coordinated monodentate (η^1) linkage in the reactant and a strongly coordinated bidentate (η^2) linkage in the rate-limiting transition structure should afford dramatic rate accelerations. Indeed, lithium diisopropylamide (LDA) dimer **1** ligated by hemi-labile amino ether **3** effects dehydrohalogenations 10^3 times faster than does dimer **4** solvated by *n*-BuOMe (eq 2).[4] The binding constants of *n*-BuOMe and

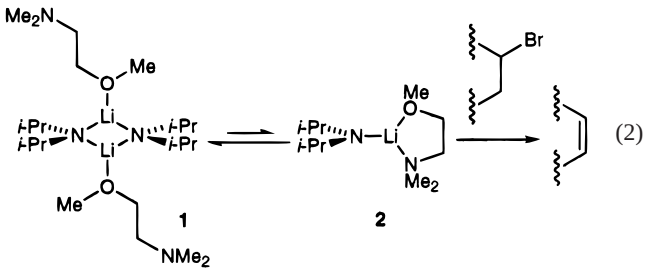

(2)

amino ether **3** were shown to be identical, and rate studies revealed that the reaction proceeds via monosolvated LDA

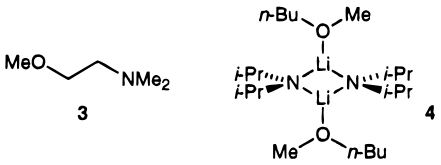

monomers in both cases. Consequently, the high rates observed when dimer **1** is used stem from stabilization of the transition structure by chelation without offsetting stabilization of the

(1) For leading references to hemi-labile ligands, see: Slone, C. S.; Weinberger, D. A.; Mirkin, C. A. *Prog. Inorg. Chem.* **1999**, *48*, 233. Bader, A.; Lindner, E. *Coord. Chem. Rev.* **1991**, *108*, 27.

(2) For example, see: Lindner, E.; Sickinger, A.; Wegner, Z. *J. Organomet. Chem.* **1998**, *349*, 75. Abu-Gnim, C.; Amer, I. *J. Mol. Catal.* **1993**, *85*, L275. Butgess, K.; Ohlmeyer, M. J.; Whitmire, K. H. *Organometallics* **1992**, *11*, 3588. Tsuda, T.; Morikawa, S.; Saegusa, T. *J. Org. Chem.* **1990**, *55*, 2978. Vineyard, B. D.; Knowles, W. S.; Sbacky, M. J.; Bachman, G. L.; Weinkauff, D. J. *J. Am. Chem. Soc.* **1977**, *99*, 5946.

(3) It is quite possible that some of the dramatic rate accelerations observed when *N*,*N*,*N*′,*N*′-tetramethylethylenediamine (TMEDA) is present stem from hemi-lability.[4] Also, see: Collum, D. B. *Acc. Chem. Res.* **1992**, *25*, 448.

(4) Remenar, J. F.; Lucht, B. L.; Collum, D. B. *J. Am. Chem. Soc.* **1997**, *119*, 5567. Remenar, J. F.; Collum, D. B. *J. Am. Chem. Soc.* **1997**, *119*, 5573.

10.1021/ja992166+ CCC: $18.00
Published on Web 11/17/1999

Scheme 1

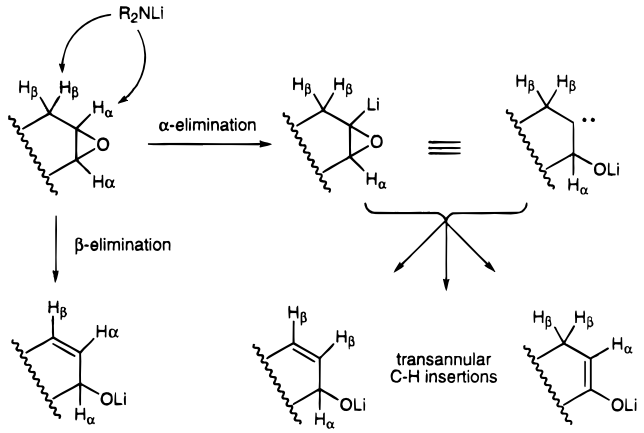

reactant. Isolating the chelate effect exclusively to the rate-limiting transition structure also eliminates the problem of deconvoluting ground state and transition state chelation effects, offering an unusually clear view of how chelation influences reactivity.

To further explore the concept of hemi-lability in organolithium chemistry, we have examined the LDA-mediated reactions of epoxides. The lithium dialkylamide-mediated rearrangements of epoxides have been investigated extensively over the past several years due to their synthetic and theoretical interest.[5,6] Both α- and *β*-metalations (Scheme 1) are known to be sensitive to the choice of substrate, lithium amide, and solvent. Deuterium-labeling experiments have confirmed the stereo- and regiochemistry of metalation in many cases.[7] Whereas the *β*-metalation (vicinal elimination) is usually implicated in the formation of allylic alcohols,[7a,c] α-metalations and the resulting oxacarbenoids[7,8] can lead to transannular C−H bond insertions to give saturated alkoxides,[9−11] vicinal C−H insertions to give lithium enolates,[12] or vicinal C−H insertions to form allylic alkoxides.[7a,d]

We describe herein rate and mechanistic investigations of three LDA-mediated epoxide rearrangements. A particularly interesting[11,13] rearrangement of *cis*-cyclooctene oxide (**5**) is shown in eq 3. Metalations of **5** using LDA solvated by

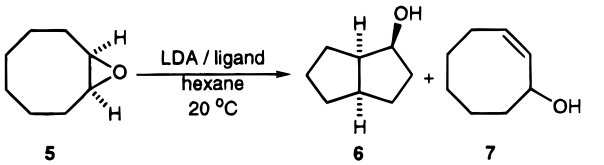

(3)

monodentate ethereal ligands such as Et_2O[11] and *n*-BuOMe afford exclusively bicyclooctane **6** very slowly. In contrast, treatment of **5** with LDA dimer **1** containing coordinated amino ether **3** in hexane rapidly affords **6** along with minor quantities of cyclooctenol **7**. Interestingly, the [**6**]:[**7**] ratio depends on the concentration of ligand **3**.

To fully understand the bifurcated pathway in eq 3 we also investigated two very clean, seemingly related eliminations: (1) the LDA-mediated elimination of epoxide **8** (eq 4), which

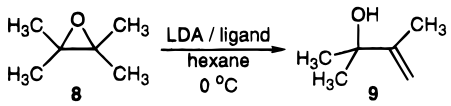

(4)

certainly proceeds via a vicinal elimination,[14] and (2) the LDA-mediated elimination of norbornene epoxide **10** (eq 5), which

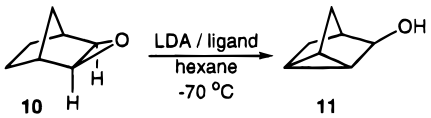

(5)

appears to proceed via an α-metalation/oxacarbenoid pathway.[10] By using both LDA/**3** and LDA/*n*-BuOMe mixtures for the eliminations in eq 3−5, we will document the origins of the regioselectivity as well as the merits of hemi-labile ligand **3**.

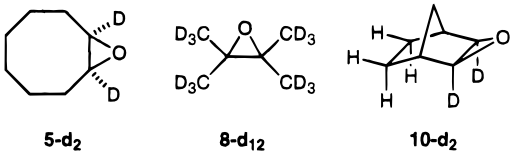

Results

General. LDA was prepared and recrystallized as described previously[15] and exists as a disolvated dimer (**1**) under all conditions studied herein.[4] Pseudo-first-order conditions were established at normal LDA concentrations (0.04−0.40 M) by restricting the epoxide concentrations to ≤0.004 M. LDA concentrations refer to the concentration of the monomer subunit (normality). The ligand concentrations refer to the concentration of free ligand by excluding lithium-bound ligand on LDA dimers **1** and **4**. The reaction rates were monitored by following loss of the epoxides and formation of products of quenched samples.

(5) Reviews: Satoh, T. *Chem. Rev.* **1996**, *96*, 3303. Crandall, J. K.; Apparu, M. *Org. React*. **1983**, *29*, 345.

(6) For leading references to asymmetric eliminations of epoxides, see: O'Brien, P. *J. Chem. Soc., Perkin Trans. 1* **1998**, 1439. Hodgson, D. M.; Gibbs, A. R.; Lee, G. P. *Tetrahedron* **1996**, *52*, 14361. Cox, P. J.; Simpkins, N. S. *Tetrahedron: Asymm.* **1991**, *2*, 1.

(7) (a) Morgan, K. M.; Gajewski, J. J. *J. Org. Chem.* **1996**, *61*, 820. (b) Crandall, J. K.; Crawley, L. C.; Banks, D. B.; Lin, L. *J. Org. Chem.* **1971**, *36*, 510. (c) Thummel, R. P.; Rickborn, B. *J. Am. Chem. Soc.* **1970**, *92*, 2064. (d) Cope, A. C.; Berchtold, G. A.; Peterson, P. E.; Sharman, S. H. *J. Am. Chem. Soc.* **1960**, *82*, 6370.

(8) Leading references to oxacarbenoids: Boche, G.; Bosold, F.; Lohrenz, J. C. W.; Opel, A.; Zulauf, P. *Chem. Ber.* **1993**, *126*, 1873. Baumgartner, T.; Gudat, D.; Nieger, M.; Niecke, E.; Schiffer, T. J. *J. Am. Chem. Soc.* **1999**, *121*, 5953.

(9) McDonald, R. N.; Steppel, R. N.; Cousins, R. C. *J. Org. Chem.* **1975**, *40*, 1694. Crandall, J. K.; Chang, L.-H. *J. Org. Chem.* **1967**, *32*, 532. Cope, A. C.; Lee, H.-H.; Petree, J. E. *J. Am. Chem. Soc.* **1958**, *80*, 2849. Cope, A. C.; Brown, M.; Lee, H.-H. *J. Am. Chem. Soc.* **1958**, *80*, 2855.

(10) Hodgson, D. M.; Lee, G. P.; Marriott, R. E.; Thompson, A. J.; Wisedale, R.; Witherington, J. *J. Chem. Soc., Perkin Trans. 1* **1998**, 2151. Hodgson, D. M.; Marriott, R. E. *Tetrahedron Lett.* **1997**, *38*, 887. Crandall, J. K. *J. Org. Chem.* **1964**, *29*, 2830.

(11) Apparu, M.; Barrelle, M. *Tetrahedron* **1978**, *34*, 1541. Boeckman, R. K. *Tetrahedron Lett.* **1977**, *49*, 4281. Whitesell, J. K.; White, P. D. *Synthesis* **1975**, 602. Cope, A. C.; Lee, H. H.; Petree, H. E. *J. Am. Chem. Soc.* **1958**, *80*, 0, 2849.

(12) Yanagisawa, A.; Yasue, K.; Yamamoto, Y. *Chem. Commun.* **1994**, 2103. Thies, R. W.; Chiarello, R. H. *J. Org. Chem.* **1979**, *44*, 1342. Bond, F. T.; Ho, C.-Y. *J. Org. Chem.* **1976**, *41*, 1421. Thummel, R. P.; Rickborn, B. *J. Org. Chem.* **1972**, *37*, 3919. Kissel, C. L.; Rickborn, B. *J. Org. Chem.* **1972**, *37*, 2060. Thummel, R. P.; Rickborn, B. *J. Org. Chem.* **1972**, *37*, 4250. Crandall, J. K.; Chang, L.-H. *J. Org. Chem.* **1967**, *32*, 435. Cope, A. C.; Trumbull, P. A.; Trumbull, E. *J. Am. Chem. Soc.* **1958**, *80*, 2844.

(13) Tierney, J. P.; Alexakis, A.; Mangeney, P. *Tetrahedron: Asymm.* **1997**, *8*, 1019. Asami, M.; Suga, T.; Honda, K.; Inoue, S. *Tetrahedron Lett.* **1997**, *38*, 6425. Also, see ref 10.

(14) Price, C. C.; Carmelite, D. D. *J. Am. Chem. Soc.* **1966**, *88*, 4039.

(15) Bernstein, M. P.; Romesberg, F. E.; Fuller, D. J.; Harrison, A. T.; Williard, P. G.; Liu, Q. Y.; Collum, D. B. *J. Am. Chem. Soc.* **1992**, *114*, 5100.

Table 1. Summary of Rate Studies for the LDA-Mediated Elimination of **5**, **8**, and **10** (Eq 1)

entry	epoxide	temp, °C	ligand	LDA order	solvent order	k_H/k_D
1	**5**	20	*n*-BuOMe	1.06 ± 0.02	-1.06 ± 0.06	2.7 ± 0.2[d]
2	**5**	20	**3**	0.92 ± 0.06[a,b] ($k_{\alpha(obsd)} + k_{\beta(obsd)}$)	-1.10 ± 0.01	3.6 ± 0.4[b]
3	**5**	20	**3**	0.85 ± 0.06[a,c] ($k_{\alpha(obsd)} + k_{\beta(obsd)}$)		2.8 ± 0.3[c]
4	**5**	20	**3**	0.94 ± 0.06[c] ($k_{\alpha(obsd)}$)	-1.11 ± 0.01[c] ($k_{\alpha(obsd)}$)	
5	**5**	20	**3**	0.95 ± 0.06[b] ($k_{\alpha(obsd)}$)		
6	**5**	20	**3**	0.61 ± 0.05[c] ($k_{\beta(obsd)}$)	-0.97 ± 0.05, 0[c,e] ($k_{\beta(obsd)}$)	
7	**5**	20	**3**	0.78 ± 0.06[b] ($k_{\beta(obsd)}$)		
8	**8**	0	*n*-BuOMe	0.51 ± 0.04	0	11 ± 1[d]
9	**8**	0	**3**	0.47 ± 0.02	0	12.3 ± 0.6
10	**10**	0	*n*-BuOMe	0.99 ± 0.06	-0.96 ± 0.05	4.3 ± 0.4[d]
11	**10**	−70	**3**	1.03 ± 0.03	-1.03 ± 0.05	6.4 ± 0.4

[a] Determined by fitting the data for loss of **5** to eq 15. [b] [**3**] = 0.5 M. [c] [**3**] = 3.0 M. [d] [*n*-BuOMe] = 0.5 M. [e] Orders correspond to dimer- and monomer-based eliminations, respectively. (See Figure 5.)

Table 2. Relative Rate Constants for the LDA-Mediated Reaction of Epoxides **5**, **8**, and **10**[a]

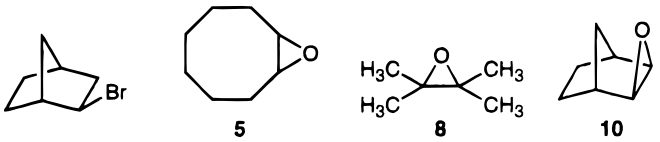

5 **8** **10**

Solvent	k_{rel}, -20 °C	k_{rel} (**6**/**7**), 20 °C	k_{rel}, 0 °C	k_{rel}, -70 °C
n-BuOMe	1.0	1.0 (>50:1)	1.0	1.0
$MeO(CH_2)_2O$-*t*-Bu	-	0.6 (>50:1)	0.9	2.4
$MeO(CH_2)_2OMe$	50	1.3 (>50:1)	1.7	3.0
$MeO(CH_2)_2N(CH_2)_5$	190	2.2 (20:1)	2.2	3.7
$MeO(CH_2)_2N(CH_2)_4$	450	9.2 (5:1)	10	38
$MeO(CH_2)_2NMe_2$	1100	30 (4:1)	22	80

[a] [LDA] = 0.1 M and [ligand] = 0.5 M in hexane.

The gas chromatographic analyses used protocols described previously.[4,16] The time-dependent loss of all three epoxides followed clean first-order kinetics, providing rate constants that are independent of the initial concentrations. Isotope effects were determined by comparing the eliminations of epoxides **5**, **8**, and **10** to the deuterated analogues **5**-d_2,[17] **8**-d_{12},[14,18] and **10**-d_2,[19] respectively, and are all consistent with rate-limiting steps involving C−H(D) bond cleavages. The rate data and isotope effects are summarized in Table 1. Representative data are depicted in Figures 1−5; additional data are included in Supporting Information.

Relative Rate Constants. The eliminations of **5**, **8**, and **10** are highly solvent dependent as shown in Table 2. (The relative rate constants are normalized to *n*-BuOMe for each substrate.) No measurable reaction is observed in the absence of an ethereal solvent. We have also included the results from the dehydrohalogenation of *exo*-norbornyl bromide[4] for comparison.

LDA/8. LDA-mediated eliminations of **8** in hexane solutions containing ligand **3** revealed a half-order dependence on the LDA concentration (Figure 1; Table 1, entry 9) and a zeroth-order dependence on the concentration of ligand **3** (Figure 2; Table 1), providing the idealized rate law in eq 6 and generalized

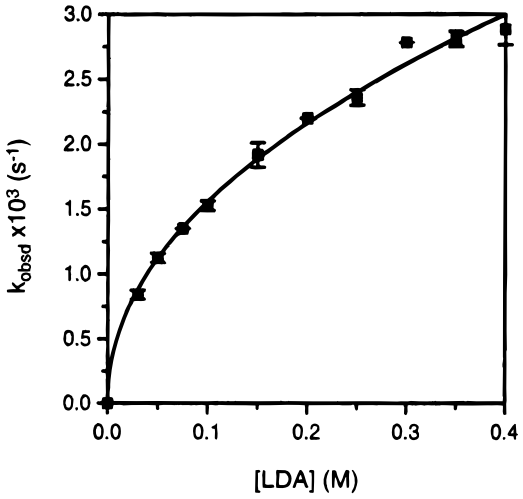

Figure 1. Plot of k_{obsd} vs [LDA] in $MeOCH_2CH_2NMe_2$ (0.5 M) and hexane cosolvent for the β-deprotonation of 2,3-dimethyl-2-butene oxide (**8**, 0.004 M) at 0 °C. The curve depicts the result of an unweighted least-squares fit to $k_{obsd} = k[LDA]^n$ ($k = 4.6 \pm 0.1 \times 10^{-3}$, $n = 0.47 \pm 0.02$).

mechanism in eqs 7 and 8. Studies using mixtures of LDA in *n*-BuOMe/hexane solutions revealed substantially reduced rates (Table 2), yet afforded an analogous rate law (eq 6, Table 1,

(16) Remenar, J. F.; Collum, D. B. *J. Am. Chem. Soc.* **1998**, *120*, 4081.
(17) Hayward, R. C.; Whitham, G. H. *J. Chem. Soc., Perkin Trans. 1* **1975**, 2267.
(18) Mazzocchi, P. H.; Klingler, L. *J. Am. Chem. Soc.* **1984**, *106*, 7567 and references therein.

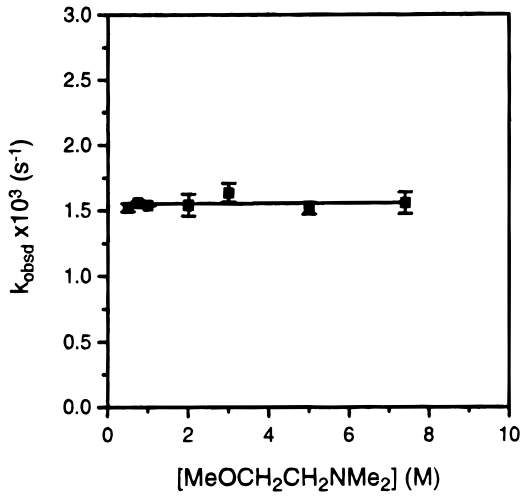

Figure 2. Plot of k_{obsd} vs [$MeOCH_2CH_2NMe_2$] in hexane cosolvent for the β-deprotonation of 2,3-dimethyl-2-butene oxide (**8**, 0.004 M) by LDA (0.10 M) at 0 °C. The curve depicts the result of an unweighted least-squares fit to $k_{obsd} = k[MeOCH_2CH_2NMe_2] + k'$ ($k = 1 \pm 7 \times 10^{-6}$, $k' = 1.55 \pm 0.02 \times 10^{-3}$).

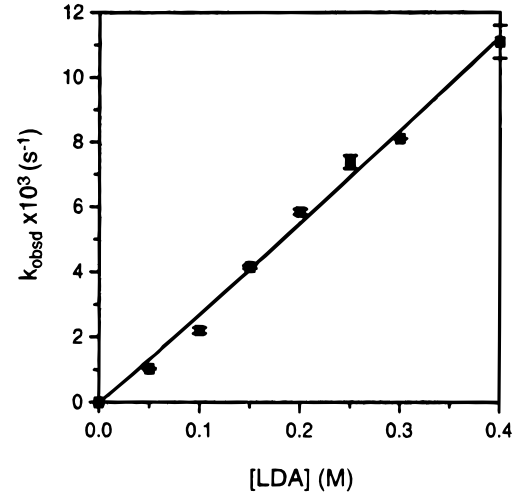

Figure 3. Plot of k_{obsd} vs [LDA] in $MeOCH_2CH_2NMe_2$ (3.0 M) and hexane cosolvent for the α-deprotonation of *exo*-norbornene oxide (**10**, 0.004 M) at −70 °C. The curve depicts the result of an unweighted least-squares fit to $k_{obsd} = k[LDA]^n$ ($k = 2.9 \pm 0.2 \times 10^{-2}$, $n = 1.03 \pm 0.05$).

entry 8) and affiliated mechanism (eqs 7 and 8).

Monomer-Based Formation of **9**:

$$-d[\mathbf{8}]/dt = k'[\text{ligand}]^0[\text{LDA}]^{1/2}[\mathbf{8}] \quad (6)$$

$$1/2\ (i\text{-Pr}_2\text{NLi})_2(\text{ligand})_2 + \mathbf{8} \rightleftharpoons (i\text{-Pr}_2\text{NLi})(\text{ligand})(\mathbf{8}) \quad (7)$$

$$(i\text{-Pr}_2\text{NLi})(\text{ligand})(\mathbf{8}) \longrightarrow \mathbf{9} \quad (8)$$

LDA/10. LDA-mediated eliminations of **10** in hexane solutions containing **3** revealed a first-order dependence on the LDA concentration (Figure 3; Table 1, entry 11) and an *inverse*-first-order dependence on the ligand concentration (Figure 4; Table 1), providing the idealized rate law in eq 9 and generalized mechanism in eq 10 and 11. Analogous studies using mixtures of LDA in *n*-BuOMe/hexane solutions revealed reduced rates (Table 2), yet afforded an analogous rate law (eq 9; Table 1,

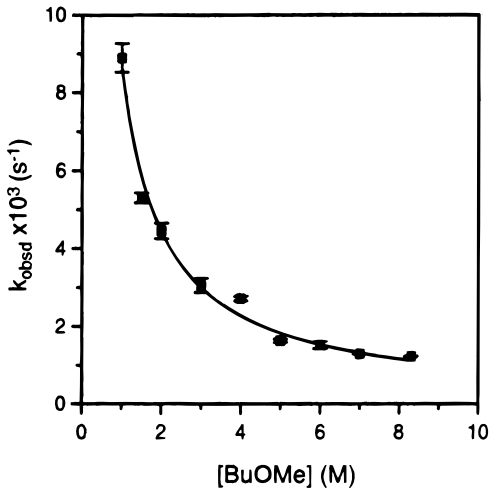

Figure 4. Plot of k_{obsd} vs [*n*-BuOMe] in hexane cosolvent for the α-deprotonation of *exo*-norbornene oxide (**10**, 0.004 M) by LDA (0.10 M) at 0 °C. The curve depicts the result of an unweighted least-squares fit to $k_{obsd} = k[n\text{-BuOMe}]^n$ ($k = 8.6 \pm 0.3 \times 10^{-3}$, $n = -0.96 \pm 0.05$).

entry 10) and affiliated mechanism (eqs 10 and 11).

Dimer-Based Formation of **11**:

$$-d[\mathbf{10}]/dt = k'[\text{ligand}]^{-1}[\text{LDA}]^1[\mathbf{10}] \quad (9)$$

$$(i\text{-Pr}_2\text{NLi})_2(\text{ligand})_2 + \mathbf{10} \rightleftharpoons (i\text{-Pr}_2\text{NLi})_2(\text{ligand})(\mathbf{10}) + \text{ligand} \quad (10)$$

$$(i\text{-Pr}_2\text{NLi})_2(\text{ligand})(\mathbf{10}) \longrightarrow \mathbf{11} \quad (11)$$

LDA/5. Eliminations of **5** with LDA/*n*-BuOMe mixtures provided exclusively bicyclooctanol **6** resulting from an α-elimination. Plots of k_{obsd} vs [*n*-BuOMe] and k_{obsd} vs [LDA] afford the idealized rate law (eq 12; Table 1, entry 1) consistent with the dimer-based mechanism described by eqs 13 and 14. This is analogous to the results for the α-metalation of substrate **10**.

Dimer-Based Formation of **6**:

$$d[\mathbf{6}]/dt = k'[\text{ligand}]^{-1}[\text{LDA}]^1[\mathbf{5}] \quad (12)$$

$$(i\text{-Pr}_2\text{NLi})_2(\text{ligand})_2 + \mathbf{5} \rightleftharpoons (i\text{-Pr}_2\text{NLi})_2(\text{ligand})(\mathbf{5}) + \text{ligand} \quad (13)$$

$$(i\text{-Pr}_2\text{NLi})_2(\text{ligand})(\mathbf{5}) \longrightarrow \mathbf{6} \quad (14)$$

The elimination of cyclooctene epoxide **5** by LDA/**3** mixtures provides two products via parallel pathways. Following loss of [**5**] vs time affords ($k_{obsd(\alpha)} + k_{obsd(\beta)}$) according to eq 15. $k_{obsd(\alpha)}$ corresponds to the pseudo-first-order rate constant for the formation of bicyclooctanol **6**, while $k_{obsd(\beta)}$ corresponds to the pseudo-first-order rate constant for the formation of cyclooctenol **7**. The [**6**]:[**7**] ratio provides $k_{obsd(\alpha)}/k_{obsd(\beta)}$, in turn, affording values for $k_{obsd(\alpha)}$ and $k_{obsd(\beta)}$.

$$[\mathbf{5}] = [\mathbf{5}]_0 \exp\{-(k_{obsd(\alpha)} + k_{obsd(\beta)})t\} \quad (15)$$

A plot of $k_{obsd(\alpha)}$ vs [LDA] ([**3**] = 3.0 M) furnishes an LDA order of 0.94 ± 0.06. A plot of $k_{obsd(\alpha)}$ vs [**3**] affords an order in ligand **3** of −1.11 ± 0.01. Taken together, the reaction orders are in reasonable accord with the idealized rate law for the formation of bicyclooctane **6** in eq 12 and the dimer-based mechanism depicted in eqs 13 and 14.

From a qualitative inspection of the data and by drawing analogy with the elimination of **8**, we anticipated that plotting $k_{obsd(\beta)}$ vs LDA and ligand concentrations would implicate a simple monomer-based mechanism for the formation of allylic

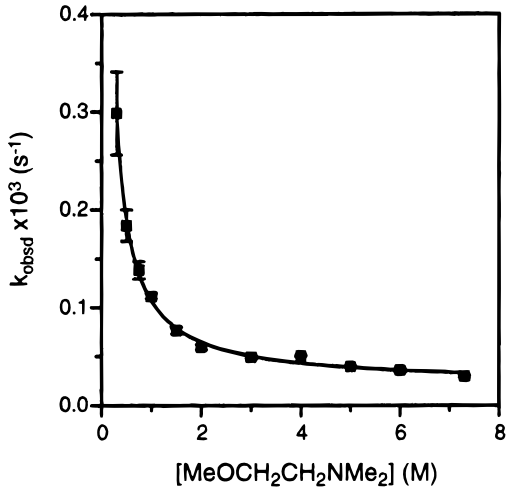

Figure 5. Plot of $k_{obsd(\beta)}$ vs [$MeOCH_2CH_2NMe_2$] in hexane cosolvent for the α- and β-deprotonation of *cis*-cyclooctene oxide (**5**, 0.004 M) by LDA (0.10 M) at 20 °C. The curve depicts the result of an unweighted least-squares fit to $k_{obsd(\beta)} = k[MeOCH_2CH_2NMe_2]^n + k'$ ($k = 8.6 \pm 0.6 \times 10^{-5}$, $n = -0.97 \pm 0.05$, $k' = 2.1 \pm 0.4 \times 10^{-5}$).

alcohol **7**. However, the results proved to be more complex than expected. A plot of $k_{obsd(\beta)}$ vs [**3**] (Figure 5) revealed evidence of a zeroth-order dependence at high ligand concentration and an inverse dependence at low ligand concentration. A plot of $k_{obsd(\beta)}$ vs [LDA] at 3.0 M concentration of **3** provides an order of 0.61 ± 0.05, a value that is slightly outside the normal range for previously measured half-order dependencies.[15,20] A plot of $k_{obsd(\beta)}$ vs [LDA] at 0.5 M concentration of **3** affords a higher LDA order (0.78 ± 0.06), indicating the emergence of a dimer-based vicinal elimination at lower ligand concentrations. We conclude that the dominant β-metalation at high ligand concentration is a monomer-based pathway as described by eqs 16−18. The inverse ligand dependence implicates a significant contribution from a dimer-based β-metalation pathway as is described by eqs 19−21. This conclusion is corroborated by

Monomer-Based Formation of **7**:

$$d[\mathbf{7}]/dt = k'[\text{ligand}]^0[\text{LDA}]^{1/2}[\mathbf{5}] \quad (16)$$

$$1/2\ (i\text{-Pr}_2\text{NLi})_2(\text{ligand})_2 + \mathbf{5} \rightleftharpoons (i\text{-Pr}_2\text{NLi})(\text{ligand})(\mathbf{5}) \quad (17)$$

$$(i\text{-Pr}_2\text{NLi})(\text{ligand})(\mathbf{5}) \longrightarrow \mathbf{7} \quad (18)$$

Dimer-Based Formation of **7**:

$$d[\mathbf{7}]/dt = k'[\text{ligand}]^{-1}[\text{LDA}]^1[\mathbf{5}] \quad (19)$$

$$(i\text{-Pr}_2\text{NLi})_2(\text{ligand})_2 + \mathbf{5} \rightleftharpoons (i\text{-Pr}_2\text{NLi})_2(\text{ligand})(\mathbf{5}) + \text{ligand} \quad (20)$$

$$(i\text{-Pr}_2\text{NLi})_2(\text{ligand})(\mathbf{5}) \longrightarrow \mathbf{7} \quad (21)$$

the fact that eliminating the excess ligand causes a dramatic rate acceleration (consistent with the dominance of the dimer-based pathway) while the [**6**]:[**7**] ratio approaches a limiting ratio of only 6:1.

The overall rate law for the conversion of epoxide **5** to **6** and **7** (eq 3) is described by eq 22. The preference for **6** at low ligand concentrations and the formation of an equimolar **6**/**7**

$$-d[\mathbf{5}]/dt = \underbrace{k'[\text{ligand}]^{-1}[\text{LDA}]^1[\mathbf{5}]}_{\text{dimer-based formation of 6}} + \underbrace{k''[\text{ligand}]^{-1}[\text{LDA}]^1[\mathbf{5}]}_{\text{dimer-based formation of 7}} + \underbrace{k'''[\text{ligand}]^0[\text{LDA}]^{1/2}[\mathbf{5}]}_{\text{monomer-based formation of 7}} \quad (22)$$

mixture at high ligand concentration (Table 2) derives from the [ligand]-dependent inhibition of the dimer-based pathways. As expected, reactions of **5**-d_2 at high [**3**] revealed a significant isotope effect accompanied by a substantial (approximately 3-fold) decrease in the [**6**]:[**7**] product ratio due to the selective inhibition of the dimer-based α-metalation(s). Metalation of **5**-d_2 at slightly sub-stoichiometric ligand concentrations (0.9 equiv per lithium) provides dramatic rate increases due to the emerging dominance of the dimer-based pathways; however, the substantial kinetic isotope effect ($k_H/k_D = 3.8 \pm 0.5$) accompanied by virtually no change in the **6**/**7** ratio strongly suggests that both **6** and **7** derive from a dimer-based α-metalation and a common intermediate.

Discussion

Lithium dialkylamide-mediated eliminations of epoxides afford a remarkably diverse range of products including allylic alcohols, homoallylic alcohols, enolates, and a variety of carbenoid-derived products.[5] Even with labeling studies[7a] and an enormous body of empirical evidence documenting the competing α- and β-metalations illustrated in Scheme 1, the solvation and aggregation events underlying these reactions are unclear.[21] The reaction of cyclooctene epoxide **5** (eq 3) offers a particularly interesting opportunity to investigate two mechanistically and synthetically interesting issues: (1) the mechanistic basis of the observed regioselectivity and (2) the accelerating influence of hemi-labile ligands (eq 2). More specifically, treatment of cyclooctene epoxide **5** with LDA solvated by amino ether **3** provides both **6** and **7**, products subsequently shown to derive from competitive α- and β-metalations (Scheme 1), and does so very rapidly when compared with the reaction of **5** with *n*-BuOMe-solvated LDA dimer **4**. For further clarification, we also investigated the isolated examples of α- and β-metalations illustrated in eqs 5 and 4, respectively. For all three cases, we investigated the consequences of competing monomer- and dimer-based pathways as well as the rate accelerations imparted by hemi-labile ligands.

Competitive Monomer- and Dimer-Based Metalations. The rate studies reveal a bifurcation between α- and β-metalation of epoxides. The β-metalations of epoxide **8** using *n*-BuOMe-solvated dimer **4** or amino ether-solvated dimer **1** follow equivalent idealized rate laws (eq 6; Table 1, entries 8 and 9), consistent with transition structures **12** and **13** based upon monosolvated LDA monomers. The importance of chelation in transition structure **13** is confirmed by the 22-fold acceleration (vide infra). In contrast, rate studies of the α-metalation of epoxide **10** by *n*-BuOMe-solvated dimer **4** or amino ether-solvated dimer **1** furnish the same idealized rate laws (eq 9) consistent with transition structures **14** and **15** based upon monosolvated LDA dimers. The importance of chelation in

(19) Stille, J. K.; Sonnenberg, F. M.; Kinstle, T. H. *J. Am. Chem. Soc.* **1966**, *88*, 4915.

(20) (a) Galiano-Roth, A. S.; Collum, D. B. *J. Am. Chem. Soc.* **1989**, *111*, 6772. (b) Bernstein, M. P.; Collum, D. B. *J. Am. Chem. Soc.* **1993**, *115*, 8008.

(21) Tobias, D.; Rickborn, B. *J. Org. Chem.* **1989**, *54*, 777.

transition structure **15** is confirmed by the 80-fold acceleration (vide infra).

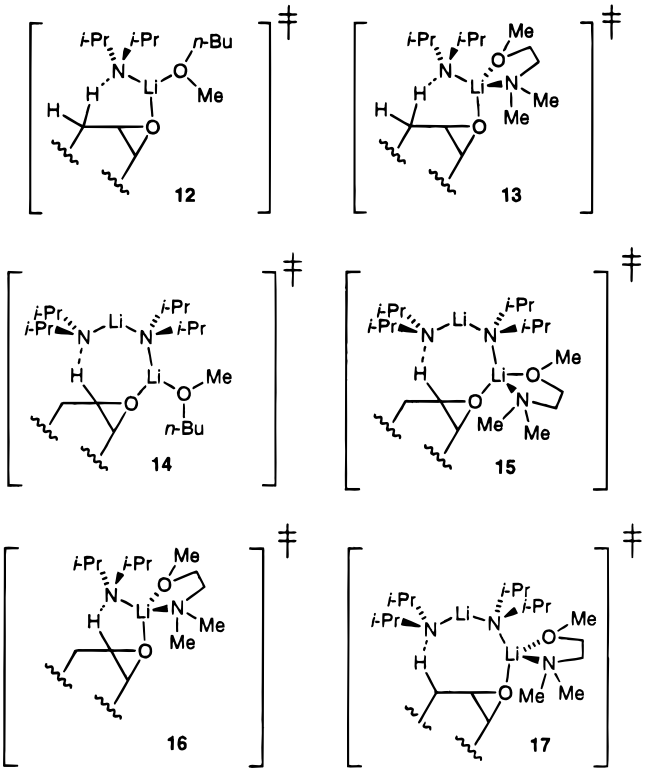

The reaction of LDA with epoxide **5** is by far the most complex of the three reactions studied, yet can be understood when supported by results from the other two case studies. Quantitative rate studies using LDA/*n*-BuOMe mixtures (LDA dimer **4**) reveal that the exclusive formation of bicyclooctanol **6** arises from an α-metalation involving a mono-solvated LDA dimer; we invoke transition structure **14** based upon the open dimer-like LDA fragment.

Analogous rate studies using both LDA/**3** mixtures (LDA dimer **1**) implicated a dimer-based α-metalation to give **6** and monomer-based *β*-metalation to give **7**. Increasing the concentrations of ligand **3** decreased the rate of consumption of **5**, decreased the [**6**]:[**7**] ratio, and increased the LDA reaction order. We observed a 3-fold decrease in the [**6**]:[**7**] ratio for **5**-d_2, further implicating competing α- and *β*-metalations. However, two predictions stemming from such a simple two-pathway model proved to be incorrect:

(1) In the absence of excess ligand, the reaction rate should increase dramatically due to the acceleration of the dimer-based pathway. The rate increases should be accompanied by the formation of **6** as the dominant (if not exclusive) product.

(2) Deconvolution of the rate constants for α-metalation ($k_{obsd(\alpha)}$) and *β*-metalation ($k_{obsd(\beta)}$) should reveal inverse-first-order and zeroth-order dependencies on the ligand concentrations, respectively.

While the overall rate at which **5** is consumed does indeed increase dramatically at sub-stoichiometric ligand concentrations, the [**6**]:[**7**] ratio approaches a limiting value of only 6:1. This suggests that there is a dimer-based pathway leading to allylic alcohol **7**. Second, a plot of $k_{obsd(\alpha)}$ vs [**3**] displays a zeroth-order dependence at high ligand concentrations, but shows an inverse dependence at low ligand concentrations. Once again, this is consistent with a measurable contribution from dimer-based formation of allylic alcohol **7** appearing at low ligand concentrations. We also found that the measured LDA order approaches that expected for a dimer-based pathway with decreasing ligand concentration.

We conclude that the bicyclooctanol **6** derives from a dimer-based transition structure, $[(R_2NLi)_2(\mathbf{3})(\mathbf{5})]^{\ddagger}$. Allylic alcohol **7** derives from primarily a dimer-based transition structure, $[(R_2NLi)_2(\mathbf{3})(\mathbf{5})]^{\ddagger}$, at low ligand concentration and a monomer-based transition structure, $[(R_2NLi)(\mathbf{3})(\mathbf{5})]^{\ddagger}$, at high ligand concentrations. The dimer-based formation of allylic alcohol **7** could proceed by either an α-metalation (via **15**) followed by oxacarbenoid insertion or a direct *β*-metalation (**17**). Indistinguishable [**6**]:[**7**] ratios observed for metalations of **5** and **5**-d_2 using sub-stoichiometric concentrations of ligand argue strongly in favor of **15** rather than **17** as the source of allylic alcohol **7**.

When taken in conjunction with the spectroscopic studies of LDA dimers **1** and **4**, kinetics only provide the *stoichiometries* of the transition structures, not the geometries. It is appropriate to comment upon some of the liberties we have taken by depicting a range of transition structures **12**−**16**. A discrete interaction of the epoxide oxygen with lithium and resulting cyclic transition structures seems intuitively logical and reasonably well-supported.[7a,22,23] As noted above and discussed more thoroughly below, the depiction of amino ether **3** as chelated in transition structures **13** and **15** is firmly supported by comparisons with *n*-BuOMe. The open dimer motifs of **14** and **15** with coordination only at the terminal lithium are well-founded by kinetic, crystallographic, spectroscopic, and computational data.[24] We will continue to depict the dimer-based reactions of lithium amides as open dimers until something shakes our confidence.

In light of the rate studies, why do the α-metalations proceed via open dimer-based transition structures such as **14** and **15** rather than a monomer-based transition structure such as **16**? The answer may be simple: angle strain. Whereas transition structures **14** and **15** may comfortably attain an approximate 180° N−H−C bond angle believed to be optimal for proton transfer,[25] transition structure **16** containing a five-membered ring certainly cannot.

On the Role of Hemi-Labile Ligands. One of the primary motivations for investigating the reactions of the epoxides with LDA was to further explore the accelerating influence of hemi-labile ligands first developed in the context of LDA-mediated dehydrohalogenations.[4] The principle of hemi-lability applied in this context is very simple: A difunctional ligand that chelates exclusively at the rate-limiting transition state allows the full benefits of chelation to be exploited *without offsetting ground-state stabilization*. To clarify the role of the chelate effect, we compared the efficacy of LDA solvated by *n*-BuOMe, amino ether **3**, and a variety of other difunctional ligands for mediating the eliminations in eqs 3−5. The relative rate constants are listed in Table 2. A critical feature of the comparisons is that the

(22) The cyclic model has received widespread attention in the deprotonation by chiral lithium amides: Whitesell, J. K.; Felman, S. W. *J. Org. Chem.* **1980**, *45*, 755. Asami, M. *Chem. Lett.* **1984**, 829. Leonard, J.; Hewit, J. D.; Ouali, D.; Simpson, S. J. *Tetrahedron Lett.* **1990**, *31*, 6703. Bhuniya, D.; Singh, V. K. *Synth. Commun.* **1994**, *24*, 375. Bhuniya, D.; DattaGupta, A.; Singh, V. K. *Tetrahedron Lett.* **1995**, *36*, 2847. Bhuniya, D.; DattaGupta, A.; Singh, V. K. *J. Org. Chem.* **1996**, *61*, 6108. Nilsson Lill, S. O.; Arvidsson, P. I.; Ahlberg, P. *Tetrahedron: Asymm.* **1999**, *10*, 265.

(23) Hilmersson, G.; Arvidsson, P. I.; Davidsson, Ö. *J. Am. Chem. Soc.* **1996**, *118*, 3539. Khan, A. Z.-Q.; de Groot, R. W.; Arvidsson, P. I.; Davidsson, Ö. *Tetrahedron: Asymm.* **1998**, *9*, 1223.

(24) For a bibliography of lithium amide open dimers, see: Remenar, J. F.; Lucht, B. L.; Kruglyak, D.; Collum, D. B. *J. Org. Chem.* **1997**, *62*, 5748. Also, see ref 16.

(25) Narula, A. S. *Tetrahedron Lett.* **1981**, *27*, 4119. Bell, R. P. *The Tunnel Effect in Chemistry*; Chapman and Hall: New York, 1980.

various solvated LDA dimers are isostructural and related by thermoneutral[4] ligand substitutions (eq 23); *significant differences in the rates or the mathematical forms of the rate laws are ascribable to differences exclusively at the rate-limiting transition structures*. This allows us to extract relative chelate stabilities at the transition structures directly from the relative rate constants without having to factor in differential ground-state stabilities.

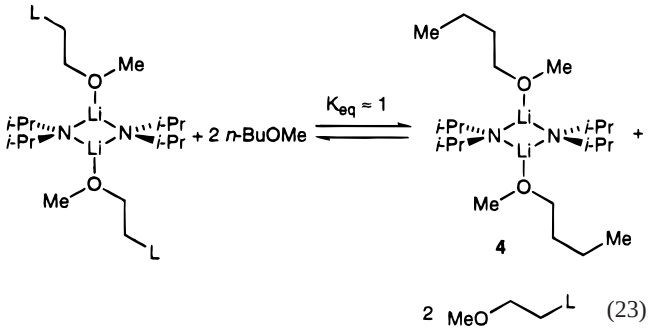

(23)

The relative rate constants listed in Table 2 offer revealing comparisons as follows:

(1) As expected, the portion of difunctional ligand, "L", that is not coordinated to the lithium of dimer **1** strongly influences the rate for all eliminations. Of special note is that the three epoxide metalations as well as the dehydrohalogenation show qualitatively the same relative ordering of reactivities. This suggests that the principles governing chelate stability at the transition structures may be general.

(2) While dimethoxyethane (DME) facilitates the dehydrohalogenation (albeit to a lesser extent than amino ether **3**), there is little evidence that DME promotes the epoxide eliminations through chelation at the transition structure. The higher azaphilicity than oxaphilicity of monomeric lithium amides (and possibly open dimers) has been noted previously.[26]

(3) The relative influences of chelation on the monomer- and dimer-based metalations (eq 24) are somewhat enigmatic. On

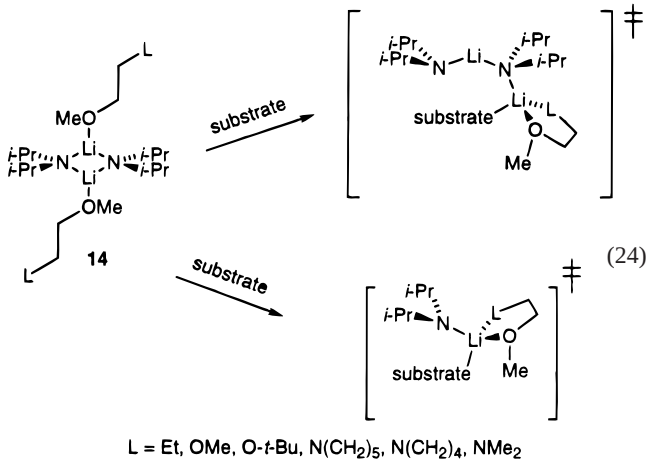

(24)

one hand, the acceleration of the putative monomer-based eliminations of **8** and that of the dimer-based eliminations of **10** are nearly equal (if the different reaction temperatures are considered). However, the ligand-dependent regioselectivities observed in the elimination of **5** (Table 2) suggest that chelation promotes the monomer-based elimination to give **7** more so than the dimer-based elimination to give **6**.

(4) The dehydrohalogenation appears to benefit more from chelation at the rate-limiting transition structure[4] than do the epoxide eliminations. We suspect that a weaker RBr−Li interaction than epoxide−Li interaction places a higher premium on the ancillary ligands.

Conclusion

The rate studies described herein show that α- and β-metalations of epoxides stem from competing dimer- and monomer-based pathways. This, in turn, offers potential strategies for the control of reaction rates and selectivities through control of these distinct pathways. As we have found on several occasions[27] and contrary to conventional wisdom, the overall reaction rates are optimal under conditions promoting the dimer-based rather than monomer-based pathways. The results also underscore the advantages offered by hemi-labile ligands in organic chemistry. Such "designer" ligands hold tremendous promise for controlling reaction rates and selectivities within organolithium chemistry.

Experimental Section

Reagents and Solvents. *cis*-Cyclooctene oxide (**5**), *exo*-norbornene oxide (**10**), *n*-BuOMe, $MeO(CH_2)_2O$-*t*-Bu, and DME were obtained from Aldrich. 2,3-Dimethyl-2-butene oxide (**8**),[14] deuterated epoxides **5**-d_2,[17] and **10**-d_2,[19] and vicinal amino ethers $MeO(CH_2)_2NMe_2$ (**3**), $MeO(CH_2)_2N(CH_2)_5$, and $MeO(CH_2)_2N(CH_2)_4$[4] were prepared according to literature procedures. 2,3-Dimethyl-2-butene oxide-d_{12} (**8**-d_{12}) was synthesized from 2,3-dimethyl-2-butene-d_{12}[18] following the procedure for the nondeuterated analogue.[14] All solvents were distilled by vacuum transfer from sodium benzophenone ketyl. The hexane still contained 1% tetraglyme to dissolve the ketyl. The LDA was prepared from *n*-BuLi (Acros) and purified by recrystallization from hexane as described previously.[15] The diphenylacetic acid used to check solution titers[28] was recrystallized from methanol and sublimed at 120 °C under full vacuum. Air- and moisture-sensitive materials were manipulated under argon or nitrogen using standard glovebox, vacuum line, and syringe techniques.

Kinetics. For a kinetic run corresponding to a single rate constant, a relatively concentrated (0.5−0.8 M) stock solution of LDA in a ligand−hexane solution was prepared and titrated to determine the precise concentration. The solution was diluted to a concentration appropriate for the particular series and titrated a second time. A series of oven-dried, nitrogen-flushed 5 mL serum vials (10 per rate constant) fitted with stir bars were charged with the LDA stock solution and brought to the desired temperature (± 0.2 °C) using a constant-temperature bath fitted with a thermometer. The epoxides were added as a 0.16 M stock solution in hexane containing dodecane (0.16 M) as a GC standard. The vessels were periodically quenched with 1:1 H_2O−THF at intervals chosen to ensure an adequate sampling of each of the first three half-lives. The quenched aliquots were extracted into Et_2O and washed with a saturated aqueous solution of NH_4Cl, and the extracts were analyzed using a Hewlett-Packard GC fitted with an autoinjector and a 60 m DB-5 column (J & W Scientific). The metalations were monitored by following the decrease of epoxides **5**, **8**, and **10** relative to the internal dodecane standard. Following the formation of the corresponding alcohols afforded equivalent rate constants within ±10%. Rate constants were determined by a nonlinear least-squares fit using the Scientist distributed by MicroMath. The reported errors correspond to one standard deviation. The observed rate constants were shown to be reproducible within ±10%.

(26) Lucht, B. L.; Bernstein, M. P.; Remenar, J. F.; Collum, D. B. *J. Am. Chem. Soc.* **1996**, *118*, 10707. Lucht, B. L.; Collum, D. B. *J. Am. Chem. Soc.* **1996**, *118*, 2217.

(27) Sun, X.; Collum, D. B. *J. Am. Chem. Soc.* **1999**, submitted for publication. Bernstein, M. P.; Collum, D. B. *J. Am. Chem. Soc.* **1993**, *115*, 789. Also, see refs 16 and 20b.

(28) Kofron, W. G.; Baclawski, L. M. *J. Org. Chem.* **1976**, *41*, 1879.

Acknowledgment. We acknowledge the National Science Foundation Instrumentation Program (CHE 7904825 and PCM 8018643), the National Institutes of Health (RR02002), and IBM for support of the Cornell Nuclear Magnetic Resonance Facility. We thank the National Institutes of Health for direct support of this work and the Spanish Ministry of Education and Culture for a postdoctoral fellowship supporting A. Ramírez.

Supporting Information Available: Tabular and graphical presentation of rate data as well as general experimental methods (PDF). This material is available free of charge via the Internet at http://pubs.acs.org.

JA992166+